Journal of Information Systems Engineering and Management
2025, 10(15s)
e-ISSN: 2468-4376
https://www.jisem-journal.com/

Research Article

Exponentially Carpet Weaving Optimization Enabled GoogleNet for Melanoma Classification using Skin Images

[1]Vijaya P, [2]Satish Chander, [3]Anisha Rodrigues, [4]Mohamed Sirajudeen Yoosef, [5]Joseph Mani, [6]Basant Kumar, [7]Hothefa Jassim

[1][4][5][6][7] Modern College of Business and Science, Bowshar, Muscat
[2] Birla Institute of Technology, Mesra, Ranchi, India
[3] NMAMIT, Karkala, Karnataka, India
Vijaya.Padmanabha@mcbs.edu.om

ARTICLE INFO

Received: 04 Dec 2024
Revised: 22 Jan 2025
Accepted: 04 Feb 2025

ABSTRACT

- Skin cancer is an invasive condition characterized by abnormal proliferation of melanocyte cells in body, where the cells can multiply and spread through lymph nodes for damaging nearby tissues. The early detection is essential for better treatment. Currently, it is widely recognized that the melanoma is the common skin cancer since it is significantly more likely to spread to other parts of the body when it is not treated or diagnosed promptly. To mitigate this challenge, an approach is proposed for melanoma classification using skin images named Exponentially Carpet Weaving Optimization enabled GoogleNet (ECWO_GoogleNet). The input skin image is pre-processed by Adaptive Kalman filter. Then, the skin lesion segmentation is performed by utilizing ENet, and then feature extraction is carried out. At last, the melanoma classification is conducted by GoogleNet, which is classified into Melanoma, Melanocytic nevus, Basal cell carcinoma, Actinic keratosis, Benign keratosis (solar lentigo / seborrheic keratosis / lichen planus-like keratosis), Dermatofibroma, Vascular lesion, and Squamous cell carcinoma. Here, GoogleNet is trained by ECWO. The analytic measures of ECWO_GoogleNet namely, Accuracy, True Positive Rate (TPR) and True Negative Rate (TNR) achieved 91.89%, 91.99%, and 91.27%.

Keywords: Skin image, Melanoma classification, Adaptive Kalman filter, ENet, GoogleNet.

I. INTRODUCTION

Skin cancer is among the most general types of cancer in the world, particularly in white populations [1]. Certain environmental as well as genetic factors like fair skin, pollution, family history, and sunburn, can contribute to the development of skin cancer. While controlling cancer-related mortality rates poses significant challenges; developments in image processing and artificial intelligence may aid earlier diagnosis of melanoma, since early detection and prognosis are important to improve the survival rates [2]. The decrease in death rate owing to skin cancer may be linked to various developments in detection and prognosis techniques. Over the past 30 years, an extensive amount of research in both domains has led to significant progress. One of the prognostic factors for cancer treatment is detection at the earliest. Recently, the developments in imaging techniques and computerized systems are providing superior diagnostic results. One of the imaging techniques employed for diagnosing skin cancer is dermoscopy, which facilitates magnified visualization of the affected skin region, revealing morphological structures that cannot be identified through naked eye. Melanoma is recognized globally as a malignant tumor and it is the fastest-growing type of skin cancer, which presents a serious health risk with high mortality rate [3].

Melanocytes, the cells accountable to produce melanin that provides color to skin, hair, and eyes. Benign melanoma is the most common moles, yet certain moles become malignant melanoma. Surgical excision remains the primary treatment for malignant melanoma and it is most effective when the lesion is predicted early before it metastasizes to other organs. Once the cancer has spread to other organs, treatment becomes more complicated, which often resulted in increased mortality rates [1]. Consequently, the early recognition of malignant melanoma lesions is vital for improving the probability of recovery. Typically, dermatologists assess the prognosis and severity of melanoma by measuring its depth utilizing biopsy. Consequently, the significance of the existing techniques

employed in earlier prognosis of disease has improved. The dissimilarity among lesioned and non-lesioned regions on melanoma skin cancer images is complicated in normal states [3]. Several investigations analyzed different Machine Learning (ML) techniques for distinct types of cancer diagnosis [4]. Certain ML models need high computational time for precise diagnosis. Deep learning (DL) has become significant for automated diagnosis of several cancer types. DL has attained superior outcomes in image classification applications. Transfer learning (TL) and data augmentation are employed for conquering the lack of data and for reducing the computational and memory requirements [5].

The contribution of this work is to design melanoma classification with skin images named ECWO_GoogleNet. Here, Adaptive Kalman filter is employed for pre-processing phase, ENet is considered for skin lesion segmentation. Then, feature extraction is performed, meanwhile the melanoma is classified by utilizing the proposed GoogleNet, where its weights are tuned utilizing ECWO. Here, ECWO is the amalgamation of Carpet Weaving Optimization (CWO) and Exponentially Weighted Moving Average (EWMA).

- **Proposed ECWO_GoogleNet for melanoma classification:** A novelty designed for melanoma classification with skin images is named as ECWO_GoogleNet. The classification of melanoma is performed using GoogleNet that is tuned using ECWO. Here, ECWO is based on the incorporation of CWO and EWMA.

The layout of remaining research are: Part 2 describes the analysis of preceding mechanisms, part 3 delivers the methodology of proposed, part 4 evaluates the outputs and part 5 concludes the novelty with future work.

II. MOTIVATION

Skin cancer is being the most prevalent cancer and accounting for over half of all cancer diagnoses worldwide. Early recognition plays fundamental part in defining the prognosis of disease, which drives our efforts. So, the investigators put their effort to design a model using hybrid algorithms by analyzing existing works.

A. Literature Survey

Ding, J., *et al.* [6] developed Two-stage ensemble method for classifying melanoma. This approach showed that the segmented images was highly enhanced the accuracy. However, it did not consider classification techniques regarding the features of dermoscopy images and integration of diverse images. Thapar, P., *et al.* [7] designed Grasshopper Optimization Algorithm enabled Convolutional Neural Network (GOA_CNN) to classify melanoma. This technique effectively determined large number of image features and it was superior to handle overfitting problem. Nevertheless, the poorly annotated or imbalanced datasets reduced the performance of model. Jaber, N.J.F. and Akbas, A., [8] introduced Binary Harris Hawk optimization enabled CNN (Binary HHO_CNN) to detect melanoma skin cancer. Even though this method improved the accuracy by including pre-and post-processing steps, the impacts on several databases require detailed evaluation. Tahir, M., N *et al.* [9] established Deep Learning-Based Skin Cancer Classification Network (DSCC_Net) for diagnosing of skin cancer. This module provided essential support to dermatologists as well as health experts for diagnosing skin cancer. However, it failed to consider and investigate the individuals with dark skin.

B. Challenges

The issues of melanoma classification performed in prior techniques are enlisted as,

- The module developed in [6] improved the prediction accuracy by combining the ensemble mechanisms. Nevertheless, the overall performance was heavily relied on training data quality.
- In [7], the module enhanced the robustness against several image disturbances like noise and variations in skin lesions. But it increased the overall complexity and require more time and resources for implementation and tuning process.
- An approach designed in [8] optimized the hyperparameters that led to faster convergence. However, it did not combine expert annotations as well as medical settings for ground truth validation for improving the reliability of results.
- Although the technique introduced in [9] learned and extracted complicated features from original dermoscopic images without the necessity for manual feature engineering, it was unable to incorporate blockchain and federated learning with deep attention module to attain more favorable outcomes.
- Melanoma is a deadliest of complete skin cancer types. DL has been shown to effectively find the patterns from images as well as signals from different application domains. However, the usage of DL in medical

image analysis was limited till date. Therefore, to overcome this issue, hybrid algorithm is proposed to classify the melanoma skin cancer.

III. PROPOSED EXPONENTIALLY CARPET WEAVING OPTIMIZATION ENABLED GOOGLENET FOR MELANOMA CLASSIFICATION

The main aim of this exploration is to propose ECWO_GoogleNet for melanoma classification using skin images. First, the input skin image acquired from the database [10], and then pre-processing is performed using Adaptive Kalman filter [11]. Next, the skin lesion segmentation is done using ENet [12], which is forwarded to feature extraction process, where the features Oriented FAST and Rotated BRIEF (ORB) [13] and statistical features [14] include mean, variance, are extracted. Finally, the melanoma is classified into Melanoma, Melanocytic nevus, Basal cell carcinoma, Actinic keratosis, Benign keratosis (solar lentigo/seborrheic keratosis/lichen planus-like keratosis), Dermatofibroma, Vascular lesion, and Squamous cell carcinoma by utilizing GoogleNet [15] that is trained using ECWO. Here, ECWO is formed by the combination of CWO [16], and EWMA [17]. Fig. 1 represents general outlook of ECWO-GoogleNet for melanoma classification.

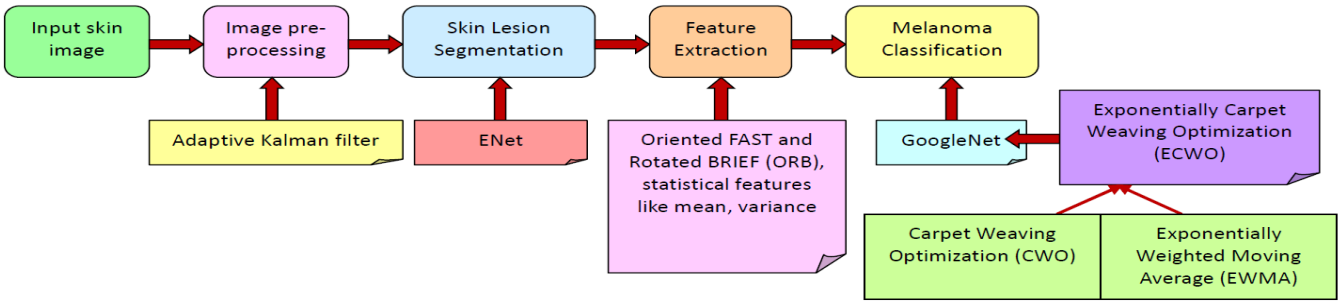

Fig. 1. General outlook of ECWO-GoogleNet for melanoma classification

A. Image Acquisition

The database used for this research has 25,331 images, available for classification task amongst nine diagnostic categories. Consider a typical database 'B' and 'd' number of the skin images is formulated by,

$$B = \{B_1, B_2, ...B_c, ...B_d\} \tag{1}$$

Here, B_c indicates input skin image and B_d represents total skin images.

B. Image pre-processing

The image B_c is forwarded to pre-processing, where the noise is reduced from the input image using Adaptive Kalman filter.

1) Adaptive Kalman filter

It is the extension of Kalman filter that adapts its factors dynamically by means of varying the characteristics of system being observed. Though the typical Kalman filter considers the linear process and constant noise characteristics, the adaptive version is introduced for handling the states where these assumptions do not hold, creating it more adaptable for real-time applications. Here, the measurement variance value is adapted to compensate for errors or inaccessible data points in the model. The objective is to random data points that are unreliable with the model to random noise by artificially improving the measurement variance so as to the data points are not utilized to corrupt the parameter evaluation [11]. The difference of measurement noise is determined by,

$$K_c = \left(\frac{1}{b}\right)\left(\sum_{a=1}^{b} \upsilon_{c-a} \upsilon_{c-a}\right) - \mathrm{H}_c^{\mathrm{T}} \mathrm{P}_c \mathrm{H}_c \tag{2}$$

Here, P_c is a covariance matrix, H_c^T is a measurement function vector, υ_c implies scalar value, b enumerates total points subsequent to a pre-defined smoothing window and a illustrates index and filtered image is specified as K_c.

C. Skin Lesion Segmentation using filtered image

It is a significant is process in medical imaging that focuses on recognizing and outlining the skin lesions within images. It aids in early detection of malignant changes, enabling prompt intervention and enhancing patient outcomes. Here, K_c is subjected as an input for segmentation, which is done by using ENet.

1) Structure of ENet

In ENet [12], the dimension of output is represented with an input resolution of 512×512. Moreover, ResNets is adopted that illustrates them with the major branch and extend with convolutional (conv) filters, which categorize them and integrate again with element-wise addition. Every block has three conv layers namely, 1×1 projection which eradicates the dimensionality, a major conv layer and 1×1 expansion. Batch Normalization and Parametric Rectified Linear Unit (PReLU) are positioned amongst overall conv layers. When the bottleneck is downsampling, a maxpooling layer is included to the major branch. Additionally, 1×1 projection is reassigned with 2×2 conv with stride 2 in both dimensions. The activations are zero padded to match the count of feature maps. The conv layer is regular, dilated or full connection with 3×3 filters. At times, it may be replaced with asymmetric conv that is a sequence of 5×1 and 1×5 conv. Spatial Dropout is utilized for regularizer with $\rho=0.01$ before the bottleneck and $\rho=0.1$ after the bottleneck. The first phase comprises only a single block. Stage 1 has 5 bottleneck blocks, while stage 2 and stage 3 have similar architecture where stage 3 does not downsample an input at initial stage. It is considered as the encoder; meanwhile the decoder considers the stage 4 and stage 5. In decoder, the maxpooling is reallocated using max unpooling as well as padding is reallocated using spatial conv without bias. Also, only a bare full convolution is decided to be place as last layer of the network that only evaluates the large-scale of decoder processing time. Here, the segmented image is signified as E_c. Fig. 2 demonstrates ENet structure, a) ENet initial block and b) ENet bottleneck model.

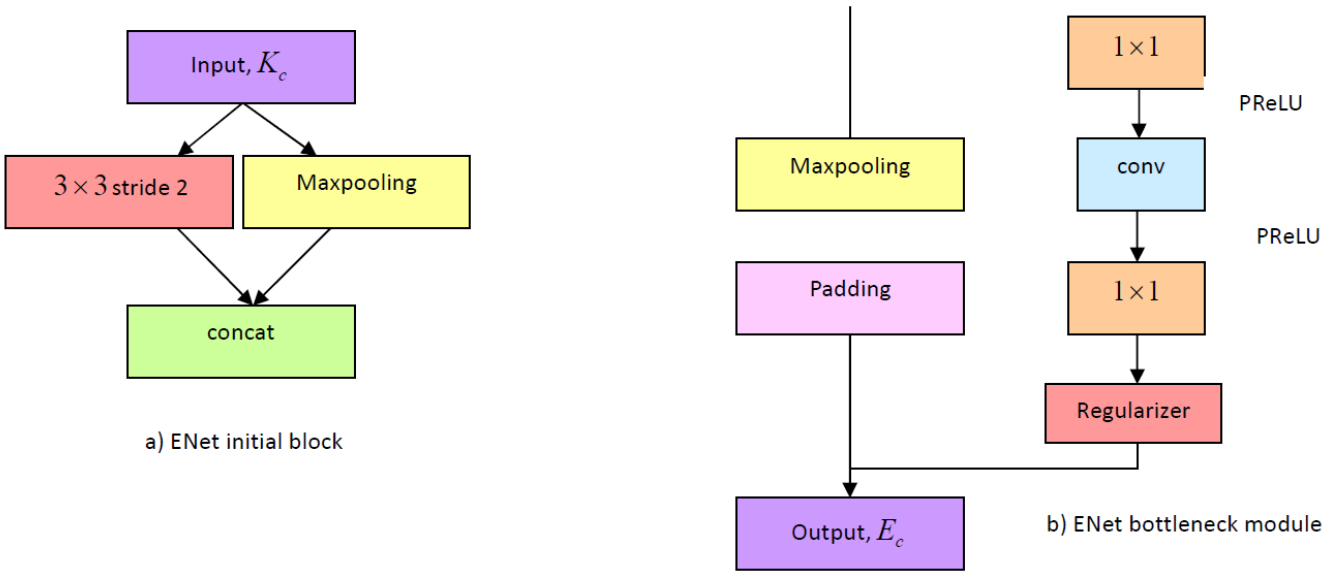

Fig. 2. Structure of ENet

D. Feature Extraction using segmented image

It is the method of classifying and quantifying relevant features from particular regions of interest within an image, which have been isolated through segmentation process. Here, E_c is forwarded as input for extracting the features.

1) ORB

ORB [13] is in excess of Scale Invariant Feature Transform (SIFT) and Speeded Up Robust Feature (SURF). It conducts the extraction process using Harris corner detector, FAST and BRIEF. It also extracts less but superior features of the image and also takes minimal computational cost. This feature results a texture feature that is enumerated as T_c. Then, this texture feature T_c is taken to attain feature vectors by applying the statistical features.

2) Statistical features

The textural feature is applied over mean and variance that is enumerated below.

a) Mean: It represents the data concentration of a distribution [14], which is determined as,

$$F_1 = \sum_{T_c=1}^{W-1} T_c * P(T_c) \tag{3}$$

Here, F_1 depicts mean, $P(T_c)$ implies probability of T_c, where T_c indicates the textural feature of every grey level image and W depicts total grey levels.

b) Variance: It expounds the divergence value of image's grey levels based on average mean grey level [14] that is determined by,

$$F_2 = \sum_{T_c=0}^{W-1} (T_c - F_1)^2 * P(T_c) \tag{4}$$

Here, F_2 defines the variance. Therefore, the resultant feature vector F_c is illustrated as,

$$F_c = \{F_1, F_2\} \tag{5}$$

E. Melanoma classification using ECWO_GoogleNet

The incidence of malignant melanoma has been rising globally. An effective non-invasive Computer Aided Diagnosis (CAD) is presented as a solution to accelerate the identification process and making it accessible to a broader population. In this module, the melanoma classification is performed using ECWO_GoogleNet with the feature vector F_c.

1) Structure of GoogleNet

GoogleNet [15] is referred as the particular version of Inception structure. By utilizing a deeper and wider Inception network, this structure demonstrated better quality. Nevertheless, integrating it into the ensemble model resulted in marginal improvements in overall outcomes. The new features of GoogleNet includes 1×1 conv, global average pooling, Inception model and auxiliary classifier for training purpose. A 1×1 conv blocks is designed for minimizing the weights and bias that led to increase the depth. The fundamental block of this network is Inception module, wherein 1×1, 3×3, 5×5 and 3×3 maxpooling corresponding performed. The resultant is concatenated and subjected to the following layer.

The general structure of GoogLeNet has 22 deep layers that is designed in Fig. 3. It considers RGB color image with dimension of 224×224 pixels as input and facilitates classification outcome as output utilizing Softmax layer. Moreover, all conv layers in this structure utilizes ReLU as activation function. The inception block in this structure is utilized for three times, which comprises 1×1, 2×2 and 3×3 dimensions. Two maxpooling of 3×3 and one global average pool are utilized. This structure observes minimal power and memory usage. The final layer of the GoogLeNet has $2048*1000$ Fully connected (FC) layers that can be varied by means of classification layers. Therefore, the classified outcome is implied as M_c.

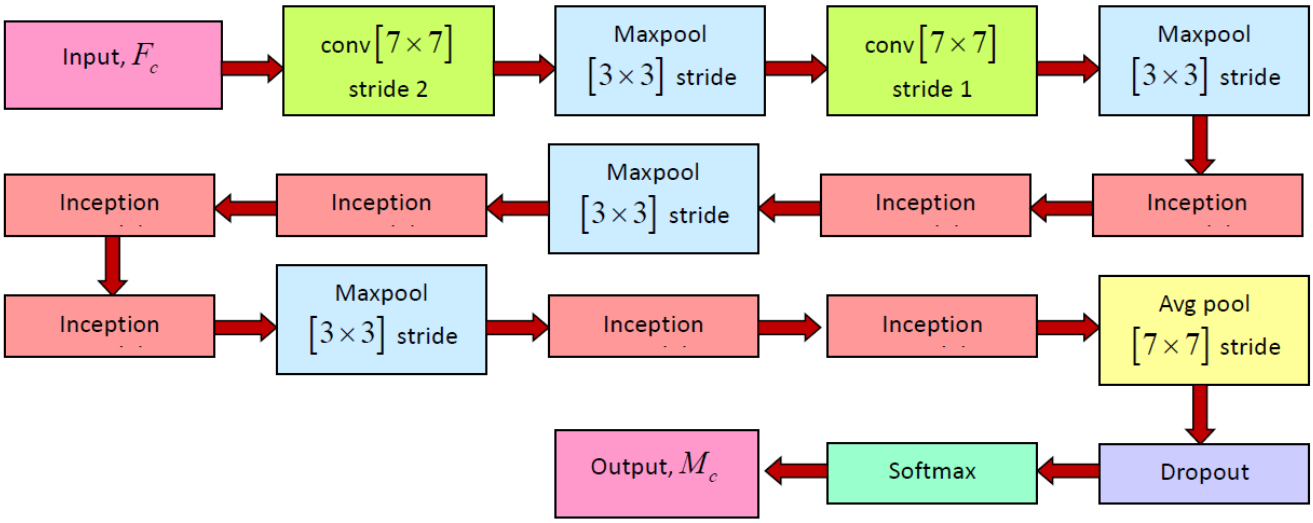

Fig. 3. GoogleNet Structure

2) Training Algorithm of GoogleNet

In this phase, the parameters of GoogleNet are trained using ECWO, which is designed by CWO and EWMA. The design of CWO [16] draws from the inspiration of the human skills in carpet weaving. It is mainly influenced by the interaction between carpet weaver and map reader, who collaborate to create a carpet based on a specified pattern. EWMA [17] is incorporated into detection techniques for providing forecasts based on trends observed in recent data, enhancing accuracy. Thus, CWO and EWMA is integrated to improve the reliability of ECWO that tunes the hyperparameters of GoogleNet effectively.

a) Solution Encoding: It defines the candidate solutions within an optimization algorithm in a certain search space (α) that is computed by $\alpha = [1\times\beta]$. Here, β expounds learning factor of GoogleNet.

b) Fitness measure: It quantifies the effectiveness of classification strategy in differentiating between the skin lesions of malignant as well as benign by utilizing,

$$\Phi = \frac{1}{d}\sum_{c=1}^{d}\left[\gamma_c - M_c\right]^2 \tag{6}$$

Here, Φ indicates fitness value, and γ_c represents targeted output.

c) Algorithm Steps: The algorithm of ECWO is demonstrated using the below steps:

Step 1: Initialization: The initial position of carpets in search space of initialization problem is totally random that is determined as,

$$R = \left\{r_1, r_2, \ldots..r_{p,t}, \ldots..r_{Q,o}\right\} \tag{7}$$

$$r_{p,t} = \mathrm{M}_t + h\cdot\left(\mathrm{N}_t - \mathrm{M}_t\right) \tag{8}$$

Here, R implies population of CWO, $r_{p,t}$ explicates t^{th} dimension in a search space, Q specifies total carpets, o signifies total decision variables, h refers to random number between $[0,1]$, $\mathrm{N}_t, \mathrm{M}_t$ indicates upper and lower bound of t^{th} dimension.

Step 2: Compute fitness: According to the position of the candidate solutions designed by each CWO member in the fitness function by Eq. (6).

Step 3: Exploration phase: Here, the crucial step in the carpet weaving process involves the carpet weaver initiates to weave according to a pattern that is read clearly by map reader. In CWO, the placement of arbitrarily generated member in problem solving space is taken as carpet weaving pattern that is represented as R_w, where

$r_{w,q} = \mathrm{M}_t + h \cdot \left(\mathrm{N}_t - \mathrm{M}_t\right)$. According to the modeling of general variations on carpet material, a new position for every member is determined as,

$$r_{p,q}^{\aleph_1} = r_{p,q} + \left(1-2h\right) \cdot \left(r_{w,q} - U \cdot r_{p,q}\right) \tag{9}$$

Consider, $r_{p,q}^{\aleph_1} = r_{p,q}\left(y+1\right)$, $r_{p,q} = r_{p,q}\left(y\right)$ and $r_{w,q} = r_{w,q}\left(y\right)$; substitute them in Eq. (9), then the equation is rewritten as,

$$r_{p,q}\left(y+1\right) = r_{p,q}\left(y\right)\left(1+2h \cdot U - U\right) + r_{w,q}\left(y\right)\left(1-2h\right) \tag{10}$$

After that, by incorporating the update solution of EWMA, the efficiency of ECWO is improved, where the solution of EWMA is computed as,

$$r_{p,q}^{\mathrm{E}}\left(y+1\right) = \eta \cdot r_{p,q}\left(y\right) + \left(1-\eta\right) r_{p,q}^{\mathrm{E}}\left(y-1\right) \tag{11}$$

$$r_{p,q}\left(y\right) = \frac{1}{\eta}\left[r_{p,q}^{\mathrm{E}}\left(y+1\right) - \left(1-\eta\right) r_{p,q}^{\mathrm{E}}\left(y-1\right)\right] \tag{12}$$

Apply Eq. (12) in Eq. (10), then it is rewritten as,

$$r_{p,q}\left(y+1\right) = \left[\frac{1}{\eta}\left[r_{p,q}^{\mathrm{E}}\left(y+1\right) - \left(1-\eta\right) r_{p,q}^{\mathrm{E}}\left(y-1\right)\right]\right] \left(1+2h \cdot U - U\right) + r_{w,q}\left(y\right)\left(1-2h\right) \tag{13}$$

Here, $r_{p,q}^{\aleph_1}$ indicates q^{th} dimension of first phase, and U specifies randomly selected value. $r_{p,q}^{\mathrm{E}}\left(y-1\right)$ and $r_{p,q}^{\mathrm{E}}\left(y+1\right)$ symbolizes the sum being set to the average of previous observation and current observation. If the above solution is not valid, then the below expression is analyzed that is expressed as,

$$R_p = \begin{cases} R_p^{\aleph_1}, & \Phi_p^{\aleph_1} \le \Phi_p \\ R_p, & else \end{cases} \tag{14}$$

Here, R_w expounds weaving pattern, $R_p^{\aleph_1}$ depicts new position for p^{th} member of first phase.

Step 4: Exploitation phase: Even though a pattern is provided for carpet preparation, carpet weavers often make small adjustments to the design, allowing their creativity to enhance the carpet's attractiveness. With respect to the simulation of these variations, a new position is determined for every population member that is expressed as,

$$r_{p,q}^{\aleph_2} = \left(1 + \frac{\left(1-2h\right)}{y}\right) \cdot r_{p,q} \tag{15}$$

$$R_p = \begin{cases} R_p^{\aleph_2}, & \Phi_p^{\aleph_2} \le \Phi_p \\ R_p, & else \end{cases} \tag{16}$$

Here, $R_p^{\aleph_2}$ symbolizes newly determined position for p^{th} member of second phase, $\Phi_p^{\aleph_2}$ indicates fitness value of second phase and y refers to total iteration.

Step 5: Re-evaluate fitness: It should be recomputed for reducing the error in the computed solution that is done using Eq. (6).

Step 6: Termination: After performing the above phases, the algorithm enters the following iteration and updating the solutions repeatedly till the last iteration for attaining fine solution.

IV. RESULTS AND DISCUSSIONS

The following sub-sections discusses the outcomes estimated from the analysis of ECWO_GoogleNet are.

A. Experimental Setup

The ECWO_GoogleNet is implemented in MATLAB.

B. Dataset description

This database [18] comprises the training data for ISIC 2019 challenge, which comprises 25,331 images available for dermoscopic image classification amongst nine diverse diagnostic categories namely, Melanoma, Melanocytic nevus, Basal cell carcinoma and so on.

C. Experimental Results

Fig. 4 articulates image Results of ECWO_GoogleNet. Fig. 4 a) indicates input image-1, Fig. 4 b) explicates filtered image-1, Fig. 4 c) expounds segmented image-1, Fig. 4 d) designs ORB feature-1, Fig. 4 e) originates output image-2, Fig. 4 f) enumerates input image-2, Fig. 4 g) specifies filtered image-2, Fig. 4 h) expounds segmented image-2, Fig. 4 i) depicts ORB feature-2, Fig. 4 j) designs output image-2.

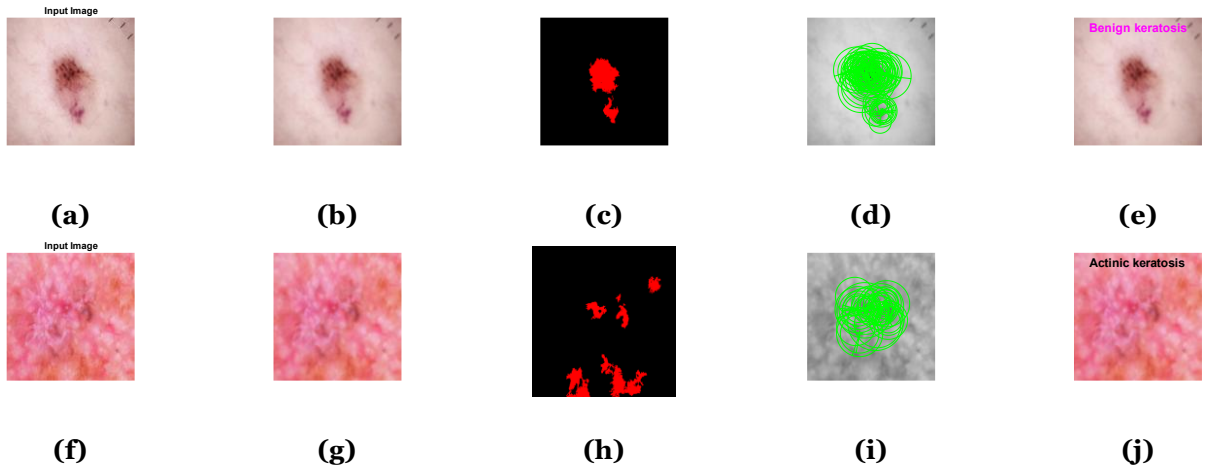

Fig. 4. Image Results of ECWO_GoogleNet, a) input image-1, b) filtered image-1, c) segmented image-1, d) ORB feature-1, e) output image-1, input image-2, g) filtered image-2, h) segmented image-2, i) ORB feature-2, j) output image-2.

D. Performance Metrics

The metrics of ECWO_GoogleNet are arranged as follows.

1) Accuracy

It is the probability of correctly classified instances to the overall instances in a database [19], which is computed by,

$$Acc = \frac{tp + tn}{tp + tn + fp + fn} \tag{17}$$

2) TPR

It is the proportion of actual positives that are correctly identified by the module [19] that is modeled by,

$$tpr = \frac{tp}{tp + fn} \tag{18}$$

3) TNR

It quantifies the proportion of actual negatives that are correctly identified [19] that is articulated by,

$$tnr = \frac{tn}{tn + fp} \tag{19}$$

Here, tp, tn, fp, fn explains true positive, true negative, false positive and false negative.

E. Comparative Methods

Two-stage ensemble method [6], GOA_CNN [7], Binary HHO_CNN [8], DSCC_Net [9] and CSBOA_TL are the comparative techniques for ECWO_GoogleNet.

F. Comparative Analysis

The ECWO_GoogleNet is executed with the different values of training data and K-fold, which is enumerated in below analysis.

1) Analysis of ECWO_GoogleNet regarding training data

By varying the value of training data with 90%, the ECWO_GoogleNet is assessed with the comparative techniques like Two-stage ensemble method, GOA_CNN, Binary HHO_CNN, DSCC_Net and CSBOA_TL are illustrated in Fig. 5. In Fig. 5 a), the ECWO_GoogleNet in terms of accuracy is represented. Here, the ECWO_GoogleNet obtained accuracy as 91.89%, where the performance improvement of ECWO_GoogleNet obtained by comparing existing approaches are 9.89%, 7.52%, 7.29%, 4.29% and 2.26%. Fig. 5 b) represents ECWO_GoogleNet evaluation regarding TPR. The ECWO_GoogleNet in terms of TPR achieved 91.99%, while comparing the traditional methods, the performance gain achieved as 13.22%, 11.77%, 10.72%, 5.82% and 3.42%. Fig. 5 c) enumerates ECWO_GoogleNet assessment in regards of TNR. The ECWO_GoogleNet based on TNR gained 91.27%, wherein previous techniques obtained 83.76%, 84.80%, 85.30%, 86.43% and 87.61%.

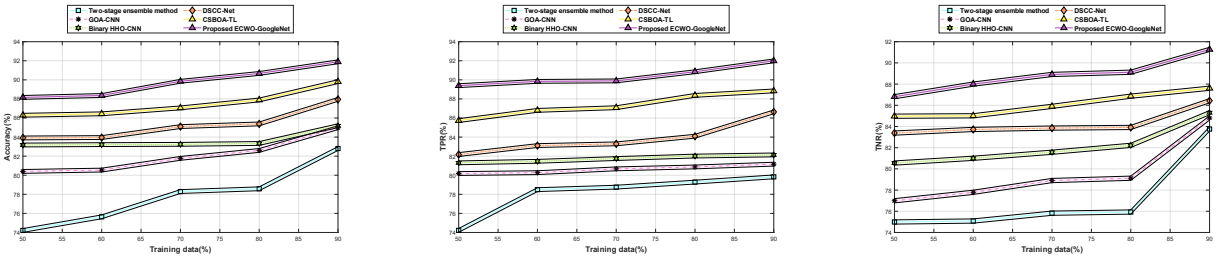

Fig. 5. Analysis of ECWO_GoogleNet regarding training data, a) Accuracy, b) TPR, c) TNR

2) Analysis of ECWO_GoogleNet regarding K-value

In this evaluation, the ECWO_GoogleNet is examined with the traditional methods namely, Two-stage ensemble method, GOA_CNN, Binary HHO_CNN, DSCC_Net and CSBOA_TL with K-value as 9, which is articulated in Fig. 6. The ECWO_GoogleNet in regards of accuracy is explicated in Fig. 6 a). Here, the ECWO_GoogleNet acquired accuracy of 91.69%, where the prior modules achieved accuracy of 81.78%, 82.52%, 84.52%, 85.40% and 89.06%. Fig. 6 b) originates ECWO_GoogleNet relating to TPR. Therefore, the ECWO_GoogleNet gained TNR with the value of 91.96%, whereas the performance improvement obtained by comparing former approaches of 10.00%, 8.86%, 7.26%, 5.85% and 4.84%. Fig. 6 c) articulates the ECWO_GoogleNet assessment in accordance of TNR. The ECWO_GoogleNet attained TNR of 91.34%, where the ECWO_GoogleNet compared with preceding methods obtained the performance gain of 7.18%, 6.70%, 5.49%, 3.935 and 2.23%.

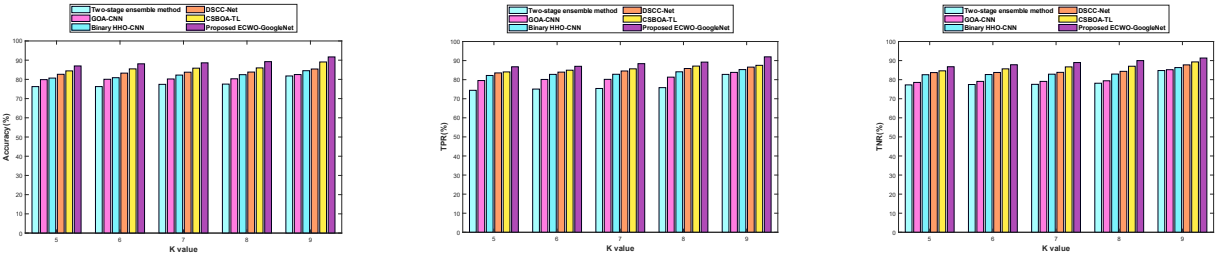

Fig. 6. Analysis of ECWO_GoogleNet regarding K-value, a) Accuracy, b) TPR, c) TNR

G. Comparative Discussions

Table I manifests the comparative values of ECWO_GoogleNet, which is attained by evaluating the existing methodologies like Two-stage ensemble method, GOA_CNN, Binary HHO_CNN, DSCC_Net and CSBOA_TL with

the proposed method. The novel approach attained maximal accuracy of 91.89% when compared with other techniques, which aids to regulate superior strategy for patient care, ensuring that those with melanoma receive timely intervention. The proposed ECWO_GoogleNet achieved highest value of 91.99%, which helps to minimize the risk of missing potentially life-threatening cases. Moreover, the TNR gained for the ECWO_GoogleNet as 91.27%. This improves the efficaciousness of population screening programs by ensuring that healthy individuals are precisely detected. The overall analysis expresses that by balancing these metrics, healthcare professionals can create a robust diagnostic tool which efficiently identifies melanoma cases by minimizing false positives, and ensuring optimal treatment strategies.

TABLE I. COMPARATIVE DISCUSSIONS

Alterations based on	Metrics/Methods	Two-stage ensemble method	GOA_CNN	Binary HHO_CNN	DSCC_Net	CSBOA_TL	Proposed ECWO_GoogleNet
Training data=90%	*Accuracy (%)*	82.80	84.98	85.19	87.95	89.81	**91.89**
	TPR (%)	79.83	81.16	82.13	86.64	88.84	**91.99**
	TNR (%)	83.76	84.80	85.30	86.43	87.61	**91.27**
K-value=9	*Accuracy (%)*	81.78	82.52	84.52	85.40	89.06	91.69
	TPR (%)	82.76	83.81	85.28	86.58	87.51	91.96
	TNR (%)	84.78	85.22	86.33	87.75	89.30	91.34

V. CONCLUSION

Skin cancer has become a significant and emerged as a global health issue, with occurrence rates rising in recent decades. The subtle variations in the skin lesions make it predominantly complicated to design an automated system for classifying benign and malignant lesions by utilizing images. Earlier identification and accurate melanoma classification are significant for effectual prognosis and it can improve patient outcomes. In this research, ECWO_GoogleNet approach is designed for classifying melanoma with the help of skin images. From the database, a particular skin image is taken for minimizing the noise in filtering process that is done using Adaptive Kalman filter. Further, ENet is employed for segmenting skin lesions and then feature extraction is done. Lastly, the melanoma is classified by utilizing GoogleNet. The parameters of GoogleNet are trained by employing ECWO, which is proposed by integrating CWO and EWMA. The evaluation metrics of ECWO_GoogleNet like accuracy, TPR, and TNR obtained utmost results of 91.89%, 91.99%, and 91.27%. In the future, smart devices equipped with CAD will systematize the diagnosis of various skin lesions.

Funded Project by MOHERI, Oman.

REFERENCES

[1] R. Indraswari, R. Rokhana, and W. Herulambang, “Melanoma image classification based on MobileNetV2 network”, Procedia computer science, vol. 197, pp.198-207, 2022.

[2] R. Kaur, H. Gholam Hosseini, R. Sinha, and M. Linden, “Melanoma classification using a novel deep convolutional neural network with dermoscopic images”, Sensors, vol. 22, no. 3, pp.1134, 2022.

[3] F. Alenezi, A. Armghan, and K. Polat, “A novel multi-task learning network based on melanoma segmentation and classification with skin lesion images”, Diagnostics, vol. 13, no. 2, pp.262, 2023.

[4] M.F. Almufareh, N. Tariq, M. Humayun, and F.A. Khan, “Melanoma identification and classification model based on fine-tuned convolutional neural network”, Digital Health, vol. 10, pp.20552076241253757, 2024.

[5] W. Salma, and A.S. Eltrass, “Automated deep learning approach for classification of malignant melanoma and benign skin lesions”, Multimedia Tools and Applications, vol. 81, no. 22, pp.32643-32660, 2022.

[6] J. Ding, J. Song, J. Li, J. Tang, and F. Guo, “Two-stage deep neural network via ensemble learning for melanoma classification”, Frontiers in Bioengineering and Biotechnology, vol. 9, pp.758495, 2022.

[7] P. Thapar, M. Rakhra, M. Alsaadi, A. Quraishi, A. Deka, and J.V.N. Ramesh, “A hybrid Grasshopper optimization algorithm for skin lesion segmentation and melanoma classification using deep learning”, Healthcare Analytics, vol. 5, pp.100326, 2024.

[8] N.J.F. Jaber, and A. Akbas, “Melanoma skin cancer detection based on deep learning methods and binary Harris Hawk optimization”, Multimedia Tools and Applications, pp.1-14, 2024.

[9] M. Tahir, A. Naeem, H. Malik, J. Tanveer, R.A. Naqvi, and S.W. Lee, “DSCC_Net: multi-classification deep learning models for diagnosing of skin cancer using dermoscopic images”, Cancers, vol. 15, no. 7, pp.2179, 2023.

[10] Skin Lesion Images for Melanoma Classification dataset will be taken from “https://www.kaggle.com/datasets/andrewmvd/isic-2019”, accessed on November 2024.

[11] S.C. Rutan, “Adaptive kalman filtering”, Analytical Chemistry, vol. 63, no. 22, pp.1103A-1109A, 1991.

[12] A. Paszke, A. Chaurasia, S. Kim, and E. Culurciello, “Enet: A deep neural network architecture for real-time semantic segmentation”, arXiv preprint arXiv:1606.02147, 2016.

[13] M. Bansal, M. Kumar, and M. Kumar, “2D object recognition: a comparative analysis of SIFT, SURF and ORB feature descriptors”, Multimedia Tools and Applications, vol. 80, no. 12, pp.18839-18857, 2021.

[14] V. Lessa, and M. Marengoni, "Applying artificial neural network for the classification of breast cancer using infrared thermographic images", In Computer Vision and Graphics: International Conference, ICCVG 2016, Warsaw, Poland, September 19-21, 2016, Proceedings vol. 8, pp. 429-438, Springer International Publishing, 2016.

[15] D. Popescu, M. El-Khatib, H. El-Khatib, and L. Ichim, "New trends in melanoma detection using neural networks: a systematic review", Sensors, vol. 22, no. 2, pp.496, 2022.

[16] S. Alomari, K. Kaabneh, I. AbuFalahah, S. Gochhait, I. Leonova, Z. Montazeri, M. Dehghani, and K. Eguchi, “Carpet Weaver Optimization: A Novel Simple and Effective Human-Inspired Metaheuristic Algorithm”, International Journal of Intelligent Engineering & Systems, vol.17, no.4, 2024.

[17] W. Febrina, and W. Fitriana, “Exponential weight moving average (EWMA) control chart for quality control of crude palm oil product”, International Journal of Management and Business Applied, vol. 1, no. 1, pp.19-27, 2022.

[18] Skin Lesion Images for Melanoma classification dataset taken from "https://www.kaggle.com/datasets/andrewmvd/isic-2019", accessed on November 2024.

[19] M. Sharma, Monika, N. Kumar, and P. Kumar, “Badminton match outcome prediction model using Naïve Bayes and Feature Weighting technique”, Journal of Ambient Intelligence and Humanized Computing, vol. 12, pp.8441-8455, 2021.